Research Article

Applied Organometallic Chemistry

Received: 5 November 2007 Revised: 21 December 2007 Accepted: 6 February 2008 Published online in Wiley Interscience:

(www.interscience.com) DOI 10.1002/aoc.1388

Electrorheology and characterization of acrylic rubber and lead titanate composite materials

N. Tangboriboon[a]*, A. Sirivat[b] and S. Wongkasemjit[b]

Oxide one-pot synthesis was used to synthesize a polymer precursor to lead titanate, $PbTiO_3$. Perovskite lead titanate, $PbTiO_3$, was synthesized via the sol–gel process. The dielectric constant, electrical conductivity and loss tangent of our acrylic rubber (AR71)–lead titanate (PT) composite material (AR/PT_8) were 14.15, 2.62 × 10^{-7}/Ω m, and 0.093, respectively, measured at 27 °C and 1000 Hz. SEM micrographs of composites between the AR71 elastomer and $PbTiO_3$ showed that the particles were reinforced within the matrix. The electrorheological properties of the AR71/PT composites were investigated as functions of electric field strength from 0 to 2 kV/mm and $PbTiO_3$ particle volume fraction. The storage modulus increased linearly with particle volume fraction, with or without an electric field. Without an electric field, the particles merely acted as a filler to absorb or store additional stress. With the electric field on, particle-induced dipole moments were generated, leading to interparticle interactions, and thus a substantial increase in storage modulus. With $PbTiO_3$ particle volume fractions as small as 10^{-4} embedded in the elastomer matrix, the modulus increased by nearly a factor of 2 as the electric field strength varied from 0 to 2 kV/mm.

Keywords: lead titanate (PT); electrorheological properties; composite material

Introduction

The sol–gel processing of glass and ceramic can dramatically lower processing costs, compared with traditional, high-temperature processing, because the same products can be obtained using lower processing temperatures and shorter times.[1] However, sol–gel processing suffers a drawback when used to process mixed-metal oxides. The wide range of hydrolysis and condensation rates of various metal alkoxides often results in chemical inhomogeneities in the gel state. These inhomogeneities may be retained in the final ceramic.[2]

Precursor processing may offer some advantages over sol–gel processing because atomic mixing relies on pre-formed chemical bonds in molecular species and the formation of a three-dimensional oxide network occurs in the last processing step instead of in an intermediate one.[3,4] However, precursor processing also often relies on expensive chemical compounds and can suffer from carbon retention in the pyrolyzed products. To overcome these problems, we have developed a synthesis route to mixed-metal alkoxide precursors directly from the oxides themselves. This approach was then extended to a one-step synthesis called oxide one-pot synthesis, or the OOPS process. This approach offers considerable potential for processing lead titanate materials.[10,11] A synthesis advantage of the oxide one-pot synthesis is the moisture-stable metal alkoxides and inexpensive starting materials. OOPS permits the low-temperature synthesis of alkaline and alkaline glycolate precursors of any stoichiometry including perovskite (ABO_3) structure.

Lead titanate (PT) in the perovskite structure (ABO_3) is an important ferroelectric material for various applications: high-energy capacitors, ultrasonic sensors, infrared detectors, and electro-optic devices.[2–7] From previous studies,[8–11] the sol–gel process appears to be the mildest method for producing lead titanate, $PbTiO_3$, ABO_3 (perovskite) structures from lead and titanium alkoxide precursors, although these precursors are moisture-sensitive.[10,11]

Ferroelectrics with various connectivity patterns, such as (0–3), (1–3) and (3–3) have been produced for many applications.[12] Of these structures, the 3–3 ferroelectric composites, in which the ceramic and polymer phases are interconnected in three directions, are also of particular interest as materials for acoustic transducers, medical imaging, muscle-like actuators, and for non-destructive evaluation.[12–14] Furthermore, the 3–3 ferroelectric composites are used to improve hydrostatic sensitivity, acoustic matching with water or human tissue, high compliance for damping, and mechanical flexibility.[12,15]

A wide variety of particulates or solid particles, such as starch, flour, silica, alumina, titania, zeolite and dielectric powders dispersed in low-conductivity non-polar matrices such as silicone, hydrocarbon oils and acrylic rubber, make up suspensions whose rheological properties can change abruptly on application of an external electric field of the order of 1 kV/mm; they are commonly known as electrorheological (ER) fluids.[16–18] The typical characteristic of ER fluids, reversible and swift transition between the liquid state and the solid state, potentially provides the most efficient approach to controlling mechanical responses by adjusting electric field strengths. The electric field-induced interactions, arising from particle polarization, is commonly believed to be responsible for ER behavior.[1–3,18] Upon application

* *Correspondence to: N. Tangboriboon, The Materials Engineering Department, Faculty of Engineering, Kasetsart University, Bangkok 10900, Thailand. E-mail: onpt@ku.ac.th*

a *The Materials Engineering Department, Faculty of Engineering, Kasetsart University, Bangkok 10900, Thailand*

b *The Petroleum and Petrochemical College, Chulalongkorn University, Bangkok 10330, Thailand*

of an electric field, the dielectric particle acquires an induced dipole and the dipole–dipole interactions cause formation of a chain-like structure of polarized particles in the direction parallel to the lines of force of the field.

The aim of this study is to prepare a high-purity $PbTiO_3$ via the sol–gel process from lead glycolate[9] and titanium glycolate[8] as the moisture-stable precursors using the OOPS process embedded in an acrylic rubber–acetone matrix. The X-ray difraction (XRD) patterns and Fourier transform infrared (FTIR) spectra of PT were investigated. $PbTiO_3$ powders[11] were added to the acrylic rubber (AR71) at various volume fractions: 0.0, 0.00002, 0.00004, 0.0002, 0.0004, 0.002, 0.004, 0.02 and 0.04. Structural and electrical properties of the ferroelectric-composite materials were investigated and are reported here. Rheological properties (G' and G'') were studied at electric field strengths in the range 0–2 kV/mm.

Experimental

Materials

Nitrogen (UHP-grade, 99.99% purity) was obtained from Thai Industrial Gases Public Company Limited (TIG). Lead acetate trihydrate 99.5 wt% $Pb(O_2CCH_3)_2{\cdot}3H_2O$ and 98 wt% NaOH were purchased from Asia Pacific Specialty Chemical Limited (Australia). Titanium dioxide was purchased from Sigma-Aldrich Chemical Co. Ltd (USA). Ethylene glycol, $HOCH_2CH_2OH$, analytical-grade EG (Farmitalia Carlo Erba, Barcelona and Malinckrodt Baker Inc., USA) was purified by fractional distillation under nitrogen at atmosphere pressure and at 200 °C before use. Triethylenetetramine (TETA) (Facai Polytech. Co. Ltd, Thailand) was distilled under vacuum (0.1 mmHg) at 130 °C prior to use. Acetonitrile and acetone (HPLC-grade) were obtained Lab-Scan Co. Ltd. The starting elastomer, acrylic rubber (AR71), was supplied by Nippon Zeon Co. Ltd, USA. The AR71 was a fast-curing type in a milk-white slab suitable for molded products like seals and gaskets. The Mooney viscosity, T_g, and specific gravity of AR71 are 50, −15 °C and 1.11 g/cm^3, respectively.

Instrumental

Fourier transform infrared spectra

FTIR were recorded on a Vector 3.0 Bruker spectrometer with a spectral resolution of 4 cm^{-1}. The composite materials were measured using the single-crystal potassium bromide, KBr. Samples were prepared as thin films.

X-ray diffraction patterns

XRD were taken and analyzed using a Phillip Electronic analyzer (NV, 1999). Samples were analyzed using a double-crystal wide-angle goniometer. Scans were measured from 10 to 80° 2θ at a scan speed of 5° 2θ/min in 0.05° or 0.03° 2θ increments using CuKα radiation ($\lambda = 0.154$ nm). Peak positions were compared with standard JCPDS files to identify crystalline phases.

Scanning electron microscopy

Micrographs were obtained using a scanning electron microscope (SEM, Jeol-5200) equipped with EDS for X-ray microanalysis. SEM samples were mounted on a stub using carbon paste and sputter coated with ~0.1 μm gold to improve conductivity.

Impedance analyzer

Electrical properties were measured and obtained using an impedance analyzer (Keithley, model 4284A), from 1 to 1000 kHz. The samples were prepared according to the ASTM B263-94 standard for electrical properties measurement. Pellet samples were prepared as thin disks having a diameter of 12 mm and a thickness of 0.50 mm. In our experiment, the electrical properties were measured at frequencies from 10^3 to 10^6 Hz.[5,19,20]

Rheometry

A controlled-strain fluid rheometer (Rheometric Scientific Inc., ARES) was used to investigate the dynamic rheological properties of the composite under controlled strain with a custom-built copper parallel plate geometry 25 mm in diameter attached to insulating spacers which were connected to the transducer or motor. Typical sample thickness or the parallel plate gap was 1.0 ± 0.1 mm. An electric field for the ER measurement was applied using a high-voltage power supply (Keithley, model 2410). Strain sweep tests were first carried out to determine the suitable strains to measure G' and G'' in the linear viscoelastic regime. Then the G' and G'' of each sample were measured as functions of frequency at various electric field strengths. The composite material samples were pre-sheared for 10 min at a low frequency (0.04 rad/s) with the electric field on in order to attain the equilibrium polarization. Each measurement was carried out at a temperature of 27 °C and was repeated at least two or three times.

Starting material preparation

Lead glycolate

Lead glycolate was synthesized via the OOPS process.[9] A mixture of lead acetate trihydrate [$Pb(O_2CCH_3)_2{\cdot}3H_2O$, 0.1 mol, 37.9 g], ethylene glycol (EG, 0.1 mol, added excess 50 cm^3) and triethylenetetramine (TETA, 0.1 mol, 14.6 g) acting as a catalyst in a round-bottom and three-necked flask (capacity, 250 cm^3) was heated at the EG boiling point under N_2 atmosphere in a thermal oil bath. The excess EG was slowly distilled off to remove water and acetic acid liberated from the reaction. After heating at 200 °C for 1 h, the solution color changed to yellow or golden brown. The reaction mixture was then cooled to precipitate a crude product, which was then filtered and washed with acetonitrile to remove any remaining ethylene glycol. A light bronze solid product was obtained and dried in a vacuum dessicator (0.1 mmHg) at room temperature.

The FTIR spectra show a peak at 2829 cm^{-1} (νC–H); 1086 and 1042 cm^{-1} (νC–O–Pb bond); and, 573 cm^{-1} (νPb–O bond). ^{13}C-solid state NMR: only a single peak at 68.6 ppm appears due to the CH_2–OH of EG as a ligand group. From the EA analysis, we found 8.864% for C and 1.392% for H, which can be compared with the calculated values of 8.990% for C and 1.498% for H. From the FAB$^+$-MS analysis, we obtained 55% intensity at the highest *m/e* 801 for [–(–$PbOCH_2CH_2O$–)$_3$–], 25% intensity at *m/e* 595 for [–$OCH_2CH_2OPbOCH_2$ $CH_2OPbOCH_2CH_2O$– + H^+], and 56% intensity at *m/e* 505 for [–$CH_2OPbOCH_2$ CH_2OPb– + H^+]. From the DSC-TGA analysis, a decomposition transition occurred from 290 to 305 °C, with a 82.5% ceramic yield corresponding to (–$PbOCH_2CH_2O$–)$_3$, obtained in terms of oligomer formation.

Titanium glycolate

Titanium glycolate was synthesized via the OOPS process as well.[8] A mixture of titanium dioxide (TiO_2, 0.025 mol, 2 g) and TETA (0.0074 mol, 3.65 g) mixed with EG (added excess 25 cm^3) was stirred vigorously and heated at the boiling point of EG under N_2 atmosphere. After 24 h, the solution was centrifuged to separate unreacted TiO_2 from the solution part. The excess EG and TETA were removed by vacuum distillation to obtain a crude precipitate. The white solid product was washed with acetonitrile and dried in a vacuum dessicator.

FTIR: 2927–2855 cm^{-1} (νC–H), 1080 cm^{-1} (νC–O–Ti bond), and 619 cm^{-1} (νTi–O bond). ^{13}C-solid state NMR: two peaks at 74.8 and 79.2 ppm appear. From EA analysis, we obtained 28.6% for C and 4.8% for H. From FAB^+-MS: 8.5% intensity at the highest *m/e* of 169 for $[Ti(OCH_2CH_2O)_2]H^+$, 73% intensity at *m/e* 94 for $[OTiOCH_2]$, and 63.5% intensity at *m/e* of 45 for $[CH_2CH_2OH]$. TGA data: one sharp transition occurs at 340 °C, and a 46.95% ceramic yield corresponding to $Ti(OCH_2CH_2O)_2$.

Lead titanate[10,11]

The lead glycolate and titanium glycolate were synthesized by the OOPS process,[7–9] whose products are less moisture-sensitive than typical metal alkoxides and the stoichiometry is easy to control.

The lead titanate sol was prepared by mixing lead glycolate in a 0.1 M nitric solution (HNO_3) with titanium glycolate to form lead titanate glycolate with a mole ratio of Pb : Ti (PT) of 1 : 1. A white turbid solution was obtained. The sol, or suspension, to semirigid gel transition occurred within a few seconds as a small amount of water was added to adjust the pH to be in the range of 3–4 at room temperature. The gels were allowed to settle at room temperature for 24 h and were dried at 50 °C for 2 days to finally obtain a light yellow gel. The lead titanate dried gels were calcined below the Curie temperature (490 °C) at 300 °C for 3 h to remove any remaining organic matter or ligand EG.[11]

$$PbCH_3(COO)_2{\bullet}3H_2O + OHCH_2CH_2OH + TETA \longrightarrow X[\text{-}(\text{-}PbOCH_2CH_2O\text{-})_3\text{-}]$$

$$TiO_2 + OHCH_2CH_2OH + TETA \longrightarrow Y[Ti(OCH_2CH_2O)_2]$$

$$X + Y \longrightarrow \text{lead titanate precursor}$$

FTIR sprectra of lead titanate: a broad peak at 3450 cm^{-1} (νO–H), smaller peaks at 1540 cm^{-1} (νC–O), two peaks at 1080 and 1042 cm^{-1} (νC–O–Pb), and at 573 cm^{-1} (νPb–O–Ti). The weight loss of the lead titanate dried gel was 25%; the percentage of ceramic yield obtained was then 75% as a result of the ethylene glycol ligand, corresponding to the theoretically calculated chemical composition 83.47 by TGA. The XRD peak patterns of the lead titanate dried gel were consistent with those of the International Center for Diffraction Data Standard (JCPDS) patterns 70-0746, 40-0099 and 70-1016. With a calcination temperature of 300 °C at 3 h, we obtained a pure tetragonal structure and a small amount of the pyrochlore phase $PbTiO_3$ [tetragonal] + $PbTi_3O_7$ [metastable]. This observation may indicate the presence of the ferroelectric perovskite phase. ^{13}C-NMR spectrum of lead titanate dried gel: one peak of ethylene glycol ligand at approximately 69 ppm appeared. An X-ray analytical microscope was used to study the mole ratio of $PbO : TiO_2$. The obtained lead titanate $PbTiO_3$ was 1.0 : 1.0 : 3.0. The data from the mass spectroscopy indicated that we obtained a molecular weight of 363 g/mol for our calcined samples. The dielectric constant, electrical conductivity and dielectric loss tangent of calcined $PbTiO_3$ were 17 470, $1.83 \times 10^{-3}/\Omega$ m, and 1.467, respectively, measured at 1000 Hz and 27 °C. The dielectric constant and electrical conductivity decreased with calcination time and temperature when it was above the limiting curve of T_c. Our synthesized materials appeared to be suitable candidates for use as electronic-grade $PbTiO_3$.

Preparation of ER solids

The lead titanate powder samples were calcined at 300 °C for 3 h. The particles were dispersed in AR71 dissolved in a 10% by volume acetone medium. The volume fractions of the PT particles dispersed in the acrylic rubber suspension studied were 0.0, 0.00002, 0.00004, 0.00020, 0.00040, 0.00199, 0.00399, 0.01965 and 0.03861 (namely AR71/PT_0, AR71/P_1, AR71/PT_2, AR71/PT_3, AR71/PT_4, AR71/PT_5, AR71/PT_6, AR71/PT_7 and AR71/PT_8 respectively). The particle size of the PT powder was 8.35±0.22 μm. Adding a large amount of lead titanate powder to the acrylic rubber AR71 resulted in a particle precipitate, or an inhomogeneous phase. The suspensions were prepared using a magnetic bar stirrer at room temperature for 24 h. The suspensions were poured into Petri dishes and allowed to dry at room temperature overnight.

Results and Discussion

FTIR characterization

The FTIR spectra of AR71/PT_8, $PbTiO_3$ powder and acrylic rubber AR71 are shown in Fig. 1, and the characteristic peaks are assigned

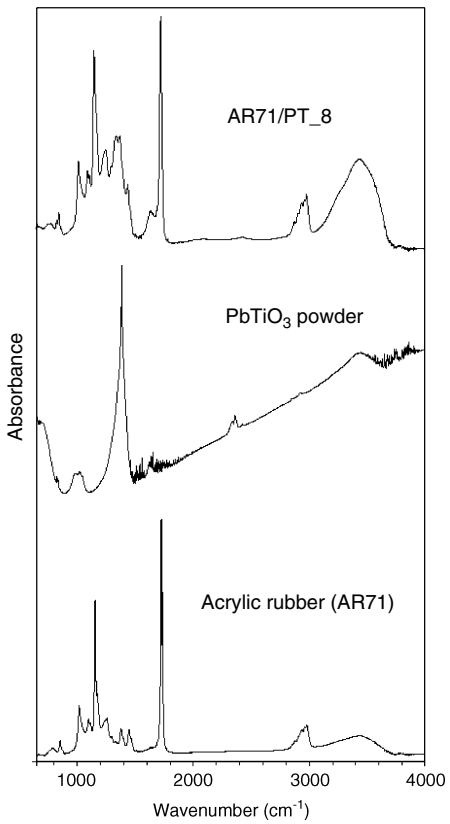

Figure 1. FTIR spectra: acrylic rubber AR71, lead titanate $PbTiO_3$ and AR71/PT_8.

Table 1. FTIR spectra of AR71/$PbTiO_3$

Wave number (cm^{-1})	Functional groups
3400 (CAS7732-18-5)	OH stretching of $PbTiO_3$ added in acrylate rubber
2980 (CAS9003-01-4)	– CH stretching vibration of $O-CH_2CH_3$
1727 (CAS79-10-7)	→ C═O stretching for carbonyl group
1446 (CAS9003-01-4)	$-CH_3$ asymmetric deformation
1379 (CAS 79-10-7)	$-CH_3$ deformation of $O-CH_2CH_3$
1257 (CAS79-10-7)	Asymmetric C–O–C stretching vibration of acrylates
1158 (CAS79-10-7)	R–CO–R symmetric stretching
1096, 1020 (CAS79-10-7)	Skeletal vibration of acrylic acid
852 (CAS9003-01-4)	C–O–C deformation

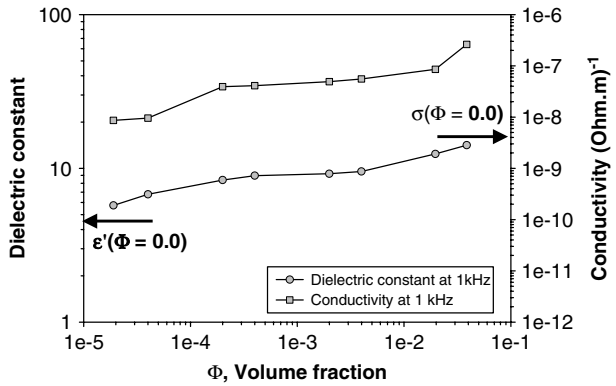

Figure 2. Electrical conductivity and dielectric constant of AR71/PT composite materials vs volume fractions.

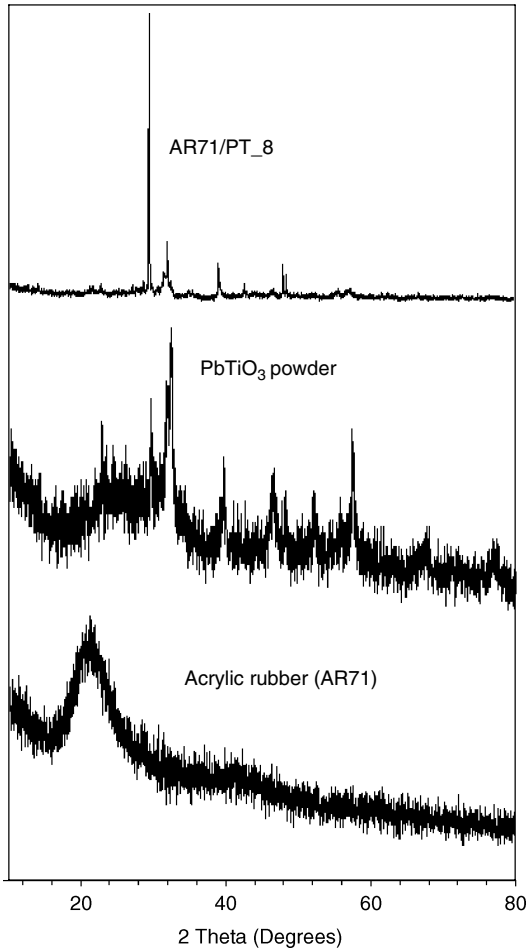

Figure 3. XRD peak patterns of acrylic rubber AR71, $PbTiO_3$ powder and AR71/PT_8.

accordingly in Table 1. The C–O–C deformation of AR71 and AR71/PT_8 shows a peak at 852 cm^{-1}. Peaks appearing at 1096 and 1020 cm^{-1} belong to the skeletal vibration of polyacrylic acid, at 1257 cm^{-1} to the asymmetric C–O–C stretching vibration of acrylates, and at 1446 cm^{-1} to the asymmetric deformation of ($-CH_3$). The carbonyl stretching exhibits two peaks, one at 1727 and one at 2980 cm^{-1}. The O–H stretching shows a broad peak at 3400 cm^{-1}. These data confirm that the acrylic rubber (AR71) in our work exhibits FTIR peaks similar to those of previously investigated thermoplastic elastomeric blends between PET and ACM.[19,21,25,26]

Electrical properties of AR71/PZT composite materials

The electrical properties of the AR71/PT composite materials were investigated using an impedance analyzer at 1 kHz, and the data are tabulated in Table 2 and shown in Fig. 2. AR71/PT_8 has the

Table 2. Electrical properties of AR71/$PbTiO_3$ measured at 27 °C and at 1000 Hz

Code	Mass of AR71 (g)	Mass of $PbTiO_3$ (g)	Volume fraction of $PbTiO_3$ (Φ)	Dielectric constant ε' at 1000 Hz	Dielectric loss factor ε'' at 1000 Hz	Conductivity $(\Omega\ m)^{-1}$, σ at 1000 Hz
AR71/PT_0	6.65993	0.0000	0.00000	4.60	0.107	4.17×10^9
AR71/PT_1	6.65999	0.0009	0.00002	5.74	0.039	8.64×10^9
AR71/PT_2	6.65997	0.0018	0.00004	6.78	0.036	9.56×10^9
AR71/PT_3	6.65990	0.0090	0.00020	8.39	0.172	3.93×10^8
AR71/PT_4	6.65970	0.0180	0.00040	8.97	0.044	4.11×10^8
AR71/PT_5	6.65870	0.0900	0.00199	9.22	0.065	4.92×10^8
AR71/PT_6	6.65338	0.1800	0.00399	9.54	0.058	5.55×10^8
AR71/PT_7	6.64668	0.9000	0.01965	12.41	0.057	8.56×10^8
AR71/PT_8	6.63360	1.8000	0.03861	14.15	0.093	2.62×10^7

Temperature, 27 °C. Density AR71 = 1.11 g/cm^3. Density $PbTiO_3$ powder = 7.50 ± 0.01305 g/cm^3.

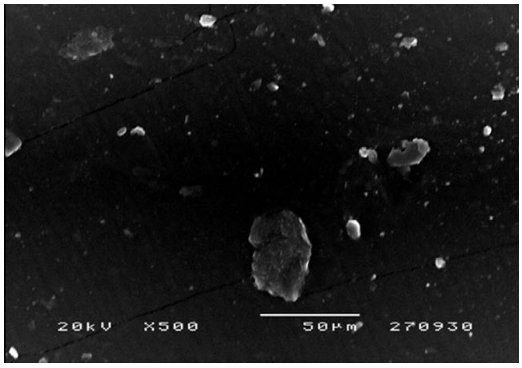

(a)

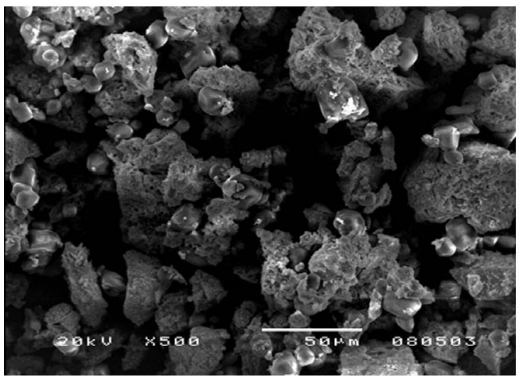

(b)

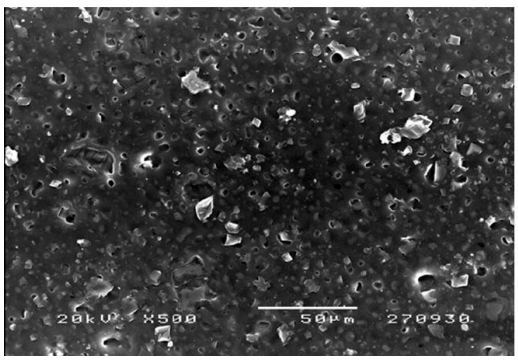

(c)

Figure 4. SEM micrographs of AR71/PT at various volume fractions at 500X: (a) pure AR71; (b) $PbTiO_3$ calcined at 300 °C for 3 h; (c) $PbTiO_3$ – doped AR71 at 300 °C for 3 h.

highest dielectric constant and electrical conductivity, 14.15 and 2.62×10^{-7} / Ω m at 1000 Hz, respectively. Both dielectric constant and electrical conductivity increase monotonically with the volume fraction of $PbTiO_3$ powder.

XRD characterization

Figure 3 shows the XRD patterns of the acrylic rubber AR71, PT powder,[15,22] and AR71/PT_8. The pattern of the AR71 indicates an amorphous structure, while the PT powder pattern suggests some crystalline structures consisting of the single-phase Perovskite-type structure mixed with a small amount of the pyrochlore phase. The X-ray peak pattern of AR71/PT_8 composite material shows a predominantly crystalline structure caused by the lead titanate powder.

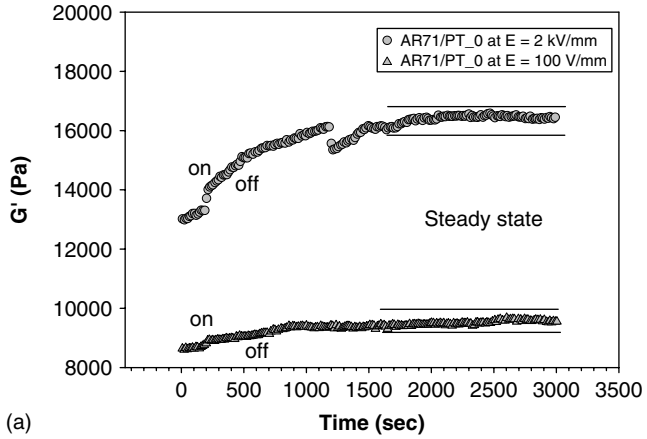

(a)

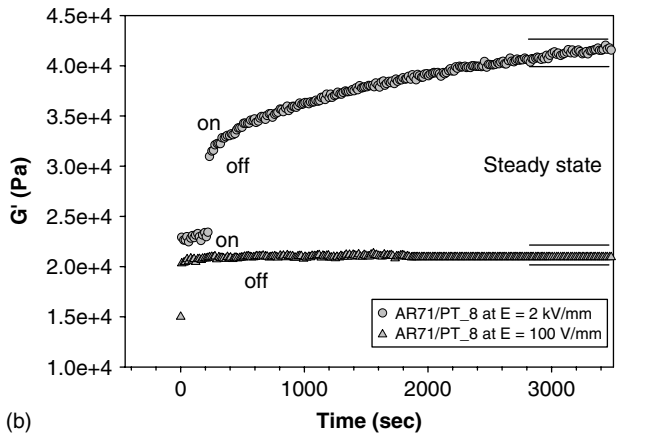

(b)

Figure 5. Temporal response of the storage modulus (G') of AR71/PT matrix at electric field strengths of 0.1 and 2.0 kV/mm, frequency 1.0 rad/s, strain 0.1%, and at 27 °C: (a) AR71/PT_0; (b) AR71/PT_8.

SEM analysis

Figure 4 shows the SEM micrographs of the acrylic rubber AR71, calcined $PbTiO_3$ and AR71/PT composite materials at a magnification of 500. $PbTiO_3$ particles appear to be moderately dispersed within the matrix. SEM micrographs of composites between AR71 elastomer and $PbTiO_3$ show that the particles are reinforced within the matrix.

Electrorheological properties: effects of particle concentration and electric field strength

Figure 5(a and b) shows the temporal characteristics of pure AR71 (AR71/PT_0) and the AR71/PT_8 at electric field strengths 0.1 and 2 kV/mm. The temporal characteristic of each sample was recorded in the linear viscoelastic regime at a strain of 0.1%, and a frequency of 1 rad/s.

Figure 5(a) shows the change in G' of the pure AR71 system, AR71/PT_0, at electric field strengths of 0.1 and 2 kV/mm during a time sweep test, in which an electric field was turned on and off alternately. At 0.1 or 2.0 kV/mm, G' immediately increased and rapidly reached a steady-state value. Then, with the electric field off, the G' decreased but did not recover its original value. Subsequent turning on and off of the electric field produced steady-state responses after a duration of about 1500 s. The response of G' can be divided into two regimes: the initial regime in which G' rapidly overshoots to a large value on the first cycle followed by an

Table 3. Rheological properties of composite materials of acrylic elastomer (Nipol, AR71) and $PbTiO_3$

Code	%v/v of $PbTiO_3$	G'_o (Pa)	$G'_{2kV/mm}$ (Pa)	G''_o (Pa)	$G''_{2kV/mm}$ (Pa)	$\Delta G'_{2kV/mm}$ (Pa)	$\Delta G'_{2kV/mm}/G'_o$
AR71/PT_0	0.00000	10,356	14,449	1,422	1,701	4,093	0.395
AR71/PT_1	0.00002	11,008	14,005	5,212	4,042	2,997	0.272
AR71/PT_2	0.00004	12,175	14,496	1,623	1,833	2,321	0.191
AR71/PT_3	0.00020	13,070	21,538	5,171	3,206	8,468	0.648
AR71/PT_4	0.00040	13,816	27,765	2,162	5,418	13,949	1.010
AR71/PT_5	0.00199	14,579	37,823	2,441	13,672	23,245	1.594
AR71/PT_6	0.00399	16,358	39,077	2,072	17,515	22,719	1.389
AR71/PT_7	0.01965	16,468	46,632	2,083	24,220	30,164	1.832
AR71/PT_8	0.03861	22,920	80,845	2,066	1,918	57,925	2.527

All materials were tested at a frequency of 1 rad/s, strain 0.1% and temperature of 27 °C; G'_o and G''_o are the storage and loss moduli without electric field; $G'_{2kV/mm}$ and $G''_{2kV/mm}$ are the storage and loss moduli at 2 kV/mm; $\Delta G'_{2kV/mm}$ is the storage modulus response defined as $G'_{2kV/mm} - G'_o$; $\Delta G'_{2kV/mm}/G'_o$ is the sensitivity of the loss modulus.

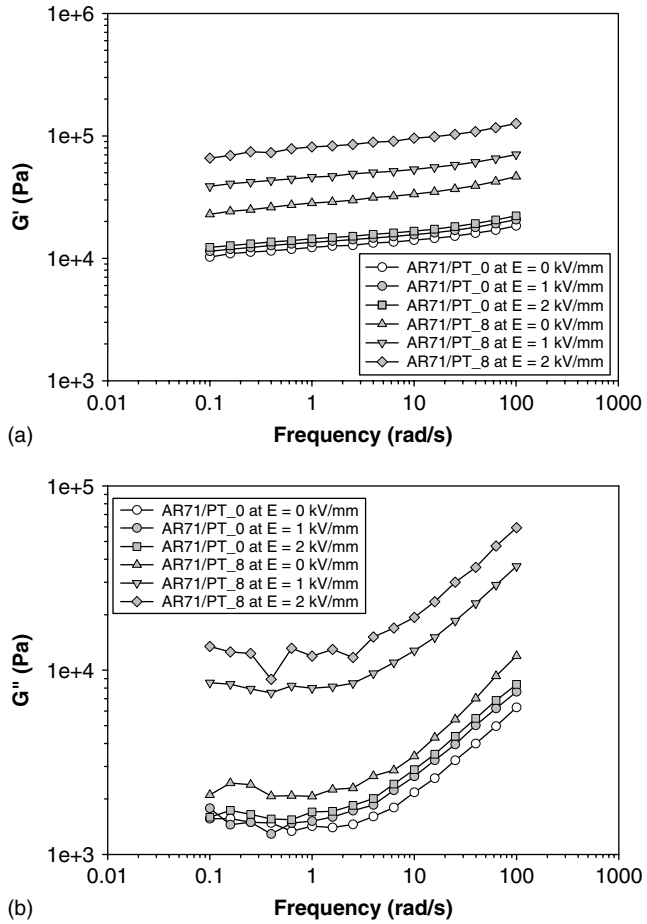

Figure 6. Moduli of AR71/PT_0 and AR71/PT_8 vs frequency at various electric field strengths: 0, 1 and 2 kV/mm, and at 27 °C: (a) storage modulus; (b) loss modulus.

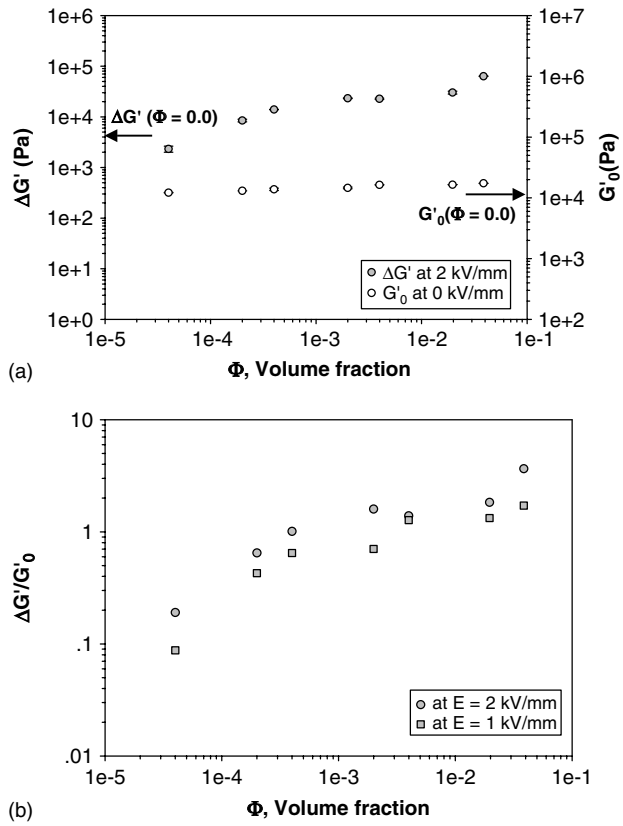

Figure 7. (a) Storage modulus response, $\Delta G'$ (1 Hz, 2 kV/mm) and G'_o (1 Hz) of the AR71/PT composite materials as functions of particle volume fraction at 27 °C. (b) $\Delta G'(\omega)/G'_0(\omega)$ of the AR71/PT composite materials as a function of particle volume fraction, at electric field strengths of 1 and 2 kV/mm, and at 27 °C.

irreversible decay with electric field off; and the steady-state regime in which G' subsequently exhibits a reversible cyclic response. The time required for G' to reach the steady-state value on applying the field is called the induction time, τ_{ind}, and the time required for G' to decay towards its steady-state value when the electric field is turned off is called the recovery time, τ_{rec}.[27,28] Figure 5(b) shows the temporal response of AR71/PT_8 at electric field strengths of 0.1 and 2.0 kV/mm, respectively. After some initial period with the electric field on and off, the AR71/PT_8 appears to be a reversible system at both of the electric field strengths. Our result here may suggest that there are some irreversible interactions among lead titanate particles, perhaps due to the dipole bondings between adjacent lead titanate particles and the residual dipole moments, inducing permanent interparticle interactions.

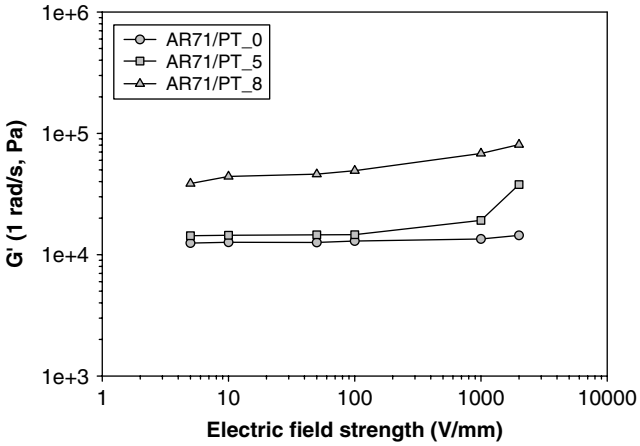

Figure 8. Storage modulus [G' (1 Hz)] of AR71/PT_0, AR71/PT_5 and AR71/PT_8 vs electric field strength, at frequency 1 rad/s, and at 27 °C.

Figure 6(a and b) shows the storage modulus (G') and the loss modulus (G'') vs frequency of AR71/PT_0 and AR71/PT_8 composite materials at electric field strengths of 0, 1, and 2 kV/mm. Both G' and G'' increased with PT particle concentration at all frequencies. Without an electric field, the storage modulus $G'(\omega)$ and the loss modulus $G''(\omega)$ of the AR71/PT_8 system were higher than those of the AR71/PT_0 system at any electric field strength. PT particles are a dielectric material in the composite materials and behave as a filler in the matrix; they can store or absorb the forces/stresses within the matrix.[22–24] A composite system with a higher particle concentration is thus expected to exhibit a higher internal stress response, a higher storage modulus $G'(\omega)$ and a higher loss modulus $G''(\omega)$ response than those of a pure acrylic rubber (AR71/PT_0) system. Without an electric field, the storage modulus G' (1 Hz) of AR71/PT_8 is $\sim 2.29 \times 10^4$ Pa. With an electric field imposed, the storage modulus G' (1 Hz) of AR71/PT_8 is 4.72×10^4 Pa and 8.09×10^4 Pa at electric field strengths of 1 and 2 kV/mm, respectively.

Figure 7(a) shows the storage modulus G'_o (1 Hz) without an electric field vs particle volume fraction and the corresponding storage response, $\Delta G'$ (1 Hz) of AR71/PT composites vs volume fraction at an electric field strength of 2 kV/mm. Both the storage modulus G'_o and the storage modulus response $\Delta G'$ appear to increase linearly with particle volume fraction from 1×10^{-5} to 1×10^{-1}. For an electric field strength of 2 kV/mm, the storage modulus response values are 4093 Pa (AR71/PT_0), 2997 Pa (AR71/PT_1), 2321 Pa (AR71/PT_2), 8468 Pa (AR71/PT_3), 13 949 Pa (AR71/PT_4), 23 245 Pa (AR71/PT_5), 22 719 Pa (AR71/PT_6), 30 164 Pa (AR71/PT_7) and 57 925 Pa (AR71/PT_8). The corresponding storage modulus sensitivity values, defined as $\Delta G'(\omega)/G'_o(\omega)$, are shown in Fig. 7(b) for AR71/PT composites; they attain G' sensitivity values of 0.395 for PT particle volume fractions of 0.0, 0.272 for 0.00002, 0.191 for 0.00004, 0.648 for 0.00020, 1.010 for 0.00040, 1.594 for 0.00199, 1.389 for 0.00399, 1.832 for 0.01965, and 2.527 for 0.03861.

The storage modulus responses, $\Delta G'$ (1 Hz) vs electric field of various composites (AR71/PT_0, AR71/PT_5 and AR71/PT_8) at a frequency of 1 rad/s are shown in Fig. 8. $\Delta G'$ (1 Hz) increases with electric field monotonically within the range 0.005–2.0 kV/mm. The storage modulus response values, $\Delta G'$ (1 Hz), of these systems at electric field strengths of 2 kV/mm are 4093, 23 245 and 57 925 Pa for AR71/PT_0, AR71/PT_5, and AR71/PT_8, respectively.

In the absence of the electric field, the PT particles are randomly dispersed within the acrylic rubber AR71 matrix and there is no particle–particle interaction. As the electrical field is applied, both PT particles and AR71 particles become polarized and induced dipole moments are generated, leading to intermolecular interactions. These intermolecular interactions induce the loss of chain-free movements and the higher chain rigidity, as indicated by higher $G'(\omega)$ values. The electric field evidently enhances the elastic modulus of our dielectric ceramic–polymer composite materials by nearly a factor of 2.

Conclusions

The lead titanate particles were synthesized via the OOPS and sol–gel process. The average particle size, dielectric constant and electrical conductivity of $PbTiO_3$ were 8.35 ± 0.22 µm, 17 470, and $1.83 \times 10^{-3}/\Omega$ m, respectively. The ER properties, G' and G'', under the oscillatory shear mode, of AR71/PT composites were investigated (with $PbTiO_3$ particle volume fractions of 0.0, 0.00002, 0.00004, 0.00020, 0.00040, 0.00199, 0.00399, 0.01965 and 0.03861) for the effects of electric field strength and particle concentration. Without an electric field, the dynamic moduli G' and G'' of each ferroelectric composite material, especially AR71/PT_8, were generally higher than those of pure acrylic rubber (AR71/PT_0) since PT particles within the matrix act as a dielectric filler; they can store or absorb the forces/stresses within the matrix. The storage modulus response increased monotonically with an electric field within the range 0.1–2.0 kV/mm. This can be attributed to the fact that the acrylic rubber (AR71) and lead titanate particles become polarized, and induced dipole moments are generated, leading to intermolecular interactions along the direction of the electric field. The storage modulus sensitivity, $\Delta G'/G'_0$, attained maximum G' sensitivity values at the electric field strength of 2.0 kV/mm of 0.395 for PT particle volume fractions of 0.0, 0.272 for 0.00002, 0.191 for 0.00004, 0.648 for 0.00020, 1.010 for 0.00040, 1.594 for 0.00199, 1.389 for 0.00399, 1.832 for 0.01965, and 2.527 for 0.03861. Our results suggest that lead titanate ($PbTiO_3$) piezoelectric particles can be used as a filler to absorb energy loss and to store additional elastic energy within the elastomer matrix. Furthermore, the lead titanate can increase the electrical properties of composite materials.

Acknowledgments

The authors would like to thank the Conductive and Electroactive Polymers Research Unit and KFAS, both of Chulalongkorn University, the Thailand Research Fund (BRG grant), the Thai Royal Government (Budget of Fiscal Year 2550), the Petroleum, Petrochemical and Advanced Materials Consortium, the Faculty of Engineering, Kasetsart University, and the Departments of Materials Engineering, Chemistry and Physics, of Kasetsart University for use of analytical equipment.

References

[1] R. Baranwal, R. M. Laine, *J. Am. Ceram. Soc.* **1997**; *80*, 1436.
[2] T. K. Mandal, S. Ram, *Mater. Lett.* **2003**; *57*, 2432.
[3] P. Kansal, R. M. Laine, *J. Am. Ceram. Soc.* **1997**; *80*, 2597.
[4] X. Junmin, J. Wang, T. Weiseng, *J. All. Com.* **2000**; *308*, 139.
[5] L. B. Kong, J. Ma, *Mater. Lett.* **2001**; *51*, 95.
[6] R. F. Zhang, J. Ma, L. B. Kong, Y. Z. Chen, T. S. Zhang, *Mater. Lett.* **2002**; *55*, 388.

[7] R. Tipakontitikul, S. Ananta, *Mater. Lett.* **2004**; *58*, 449.
[8] N. Phonthammachai, T. Chairassameewong, E. Gulari, A. Jamieson, S. Wongka semjit, *J. Metals. Min. Mater. Chulalongkorn Univ.* **2002**; *12*, 23.
[9] N. Tangboriboon, A. Jamieson, A. Sirivat, S. Wongkasemjit, *Mater. Chem. Phys.* **2006**; *98*, 138.
[10] N. Tangboriboon, A. M. Jamieson, A. Sirivat, S. Wongkasemjit, *Appl. Org. Chem.* **2006**; *20*, 886.
[11] N. Tangboriboon, A. M. Jamieson, A. Sirivat, S. Wongkasemjit, *Appl. Org. Chem.* **2007**; *22*, 104.
[12] C. J. Dias, D. K. Das-Gupta, *IEEE Trans. Die. Elect. Insul.* **1996**; *3*, 706.
[13] H. Kara, R. Ramesh, R. Stevens, C. R. Bowen, *IEEE Trans. Ultrason. Ferroelectr. Freq. Control.* **2003**; *50*, 289.
[14] R. H. Baughman, *Syn. Met.* **1996**; *78*, 339.
[15] D. Xia, M. Liu, Y. Zeng, C. Li, *Mater. Sci. Engng B* **2001**; *87*, 160.
[16] T. Hao, Z. Xu, Y. Xu, *J. Colloid Interface Sci.* **1997**; *190*, 334.
[17] T. Shiga, *Adv. Polym. Sci.* **1997**; *134*, 133.
[18] M. Parthasarathy, D. J. Klingenberg, *Mater. Sci. Engng Res.* **1996**; *17*, 57.
[19] R. Thomas, S. Mochizuki, T. Mihara, T. Ishida, *Mat. Lett.* **2003**; *57*, 2007.
[20] W. C. Las, P. D. Spagnol, M. A. Zaghete, M. Cilense, *Ceram. Int.* **2001**; *27*, 367.
[21] A. Abreu Jr., S. M. Zanetti, M. A. S. Oliveira, G. P. Thin, *J. Eur. Soc.* **2005**; *25*, 743.
[22] M. Kakihana, T. Okubu, M. Arima, O. Uchiyama, M. Yashima, M. Yuchimura, *Chem. Mater.* **1997**; *9*, 451.
[23] P. Hiamtup, A. Sirivat, A. M. Jamieson, *J. Coll. Interface Sci.* **2006**; *295*, 270.
[24] E. Shivakumar, C. K. Das, E. Segal, M. Narkis, *Polymer* **2005**; *46*, 3363.
[25] V. Pavlinek, O. Quadrat, B. Porsch, P. Saha, *Colloid Surf. A: Phys. Engng. Asp.* **1999**; *155*, 241.
[26] A. Jha, A. K. Bhowmick, *Polymer* **1997**; *38*, 4337.
[27] V. Vijayabaskar, S. Bhattacharya, V. K. Tikku, A. K. Bhowmick, *Radiat. Phys. Chem.* **2004**; *71*, 1045.
[28] T. Puvanatvattana, D. Chotpattananont, P. Hiamtup, S. Niamlang, R. Kunanuruk Sapong, A. Sirivat, A. M. Jamieson, *Rea. Fund. Polym.* **2006**; *66*, 1575.

